Proceedings Paper:

Khalfan, AMM, Andrews, GE orcid.org/0000-0002-8398-1363 and Li, H orcid.org/0000-0002-2670-874X (2017) Real World Driving: Emissions in Highly Congested Traffic. In: Proceedings of the SAE Powertrain Fuels and Lubricants Meeting 2017. SAE 2017 International Powertrains, Fuels & Lubricants Meeting, 16-19 Oct 2017, Beijing, China. SAE International .

Real World Driving: Emissions in Highly Congested Traffic

Ahmad M.M. Khalfan, Gordon E. Andrews and Hu Li
School of Chemical and Process Engineering,
University of Leeds, Leeds, UK.

Presented at the SAE International Powertrain Fuels and Lubricants Meeting

Beijing, October 16 – 18, 2017

Published in the Proceedings of the SAE Powertrain Fuel and Lubricant Meeting 2017

Abstract

The emissions from vehicles in real world driving are of current concern, as they are often higher than on legislated test cycles and this may explain why air quality in cities has not improved in proportion to the reduction in automotive emissions. This has led to the Real Driving Emissions (RDE) legislation in Europe. RDE involves journeys of about 90km with roughly equal proportion of urban, rural and motorway driving. However, air quality exceedances occur in cities with urban congested traffic driving as the main source of the emissions that deteriorate the air quality. Thus the emissions measured on RDE journeys may not be relevant to air quality in cities. A Temet FTIR and Horiba exhaust mass flow measurement system was used for the mass emissions measurements in a Euro 4 SI vehicle. A 5km urban journey on a very congested road was undertaken 29 times at various times so that different traffic congestion was encountered. Each journey was split into ten sections in order that the location and traffic conditions of the highest emissions could be determined. It was found that low speed stop-start traffic has much higher emissions than for freely moving traffic and most of the higher emissions on the longer 5km journeys occurred in relatively short sections of slow moving stop/start traffic. The journey used passed a roadside air quality monitor that exceeded the EU NO_2 and PM standards on an annual basis and it was located by the most congested part of the route, where the traffic emissions are shown in this work to be at their highest.

Introduction

Real world driving uses different powers, different average speeds, different traffic congestion conditions, different road gradients, different maximum acceleration rates, different cold start conditions, different numbers of stop/start events and occurs at different ambient temperatures and pressures than on test cycles and will inevitably have different emissions, as all these factors influence the emissions. This applies equally to spark ignition and diesel engines [1-11]. This work concentrates on the influence of real world congested traffic on vehicle movement and SI vehicle emissions.

The City of Leeds has carried out a traffic and congestion study for the whole of Leeds together with air quality monitoring across Leeds [12-14]**.** The road studied in the present work was part of this city of Leeds study, so the traffic flows for this road for specific times of the day were taken as the traffic flows during the period the vehicle emissions were measured. The air quality at several locations across the city was monitored and compared with traffic emission modelling predictions. These modelled results were based on traffic counts and the certified emissions on the NEDC test cycle. The modelled NO_2 concentration, at the roadside site in the middle of the present road journey, was 47% lower than the measured results and 28% lower for the city centre site [12, 15-17]. The NO_2 measurements showed 14 sites in Leeds above the EU limit where the model only predicted 4 sites in exceedance. The high NO_2 in the studied area was attributed to traffic congestion, as there were no local industrial air pollution sources.

Leeds has a population of 750,000 and there are 100,000 jobs in the city centre and 500,000 jobs in total within the city boundaries. At peak commuting times there were 1000 cars per hour per lane travelling into the centre of Leeds on the road investigated in this work [12-14, 17]. This road is one of five major radial routes from the north of the city into the centre, but is the most congested. The road passes two universities and two high schools just south of the test section, with a combined student and staff population of 100,000. There are also several towns to the north of Leeds that feed commuting traffic into Leeds down the road investigated.

Legislated test cycles such as the NEDC and FTP75 were not designed to produce data for air quality modelling, but to compare cars A, B, C etc. with a reference standard, on identical test cycle basis. However, it is important that the test cycle is representative of real world driving with cold start, stop/starts, acceleration and deceleration, and transient operation comparable to real world driving. This is why purely steady state testing ceased to be the only method of emissions testing for heavy duty vehicles in 2000 and was abandoned for fuel economy testing for passenger cars in 1993 in Europe and in the 1970s in the USA. However, if the test cycle conditions are well removed from current real world driving, then there is concern that the emissions on the legislated test cycle may be unrepresentative of real world driving and result in air quality not being improved as intended. This has led to the development of the WLTC test procedures and real world emissions measurement using portable emissions measurement systems (PEMS) [15-17] or Real Driving Emissions test procedures (RDE) [18-20]. The intention was that these new test cycles were more representative of real world driving. However, it will be shown in this work that they are not representative of real world congested traffic driving, which is responsible for most urban air quality exceedances.

Table 1 compares some key test parameters between the test cycles, typical RDE data, which are mainly taken from Hausberger et al [18], and the present congested traffic route using the whole journey emissions data [17]. The severity of congestion in traffic is represented by the average velocity of the traffic. However, the average velocity is limited by the speed limit of particular roads. So a common congestion factor, CF, is used for the indication of congestion, defined as follows:

$$CF\ \% = 100\ [1 - (\text{Ave. Speed} / \text{legal speed limit})] \quad (1)$$

It is generally regarded that the traffic is significantly congested if the CF is less than 50%, i.e. the average speed of a journey is lower than the half of the speed limit of the road. If the CF is 0, it means that the average speed is equal to the speed limit of the road, i.e. no congestion. In this case a vehicle can travel at the maximum allowed speed with no influence of other traffic or of road junctions. The average velocity was determined by the time taken to travel a specified distance in the traffic, using the present vehicle in the traffic flow. It was also the same as the average of the instantaneous measured velocities. In the Leeds city council work [12-14] the average time of a vehicle travelling 3.5 km on this road in the same direction was determined. The present test route was in the middle of the test section used by Leeds City Council and hence the traffic

Table 1. Comparison of key parameters in test cycles and in real world driving

Test Cycle	NEDC	FTP	JC09	WLTC	RDE [18-20]	[17]
Mean Vel. km/h	33.6	31.5	24.4	46.5	30-110	5–26
CF%	30%	34%	49%	3%	0%	46-90%
Max. Acc. m/s^2	1.0	1.5	1.7	1.7	1.5	2.2–2.8
Dist., km	11	12	8.2	23.3	80-90	5
No. Acc. from Idle /km	1.3	1.5	1.5	0.4	~0.2	1.4-7
Idle time %	23.7	17.6	28.7	12.6	~0	20-57

flows were assumed to be the same for the same time of day. The average velocity over the 3.5 km route was determined from the measured time of travel of a vehicle in the traffic flow [17]. In the present work the average velocity was the length of each section of the journey divided by the time taken to complete that section of the journey.

Another factor of importance in congested traffic is the number of stop/starts per km, which is related to the number of accelerations from idle per km (No. acc. from idle/km). This is a key feature of the NEDC, FTP75 and JC09 test cycles but is absent from the WLTC and RDE apart from at the start. However, Table 1 shows that in the work of Khalfan et al. [17] congested traffic had a minimum number of accelerations from idle per km, at the lowest congestion tested, of 1.4/km and this is similar to that in the NEDC, FTP75 and JC09. However, as congestion increases so does the number of accelerations from idle and were 7/km (170m average distance between stops) for the highest congestion in the work of Khalfan et al. [17] for the whole of the present journeys.

It is shown in the present work that in the section of the journey by a roadside air quality monitor the number of stop/starts was as high as 17/km for the most congested traffic. This is on average a stop/start every 60m and this was occurring in the section of the journey next to the roadside air quality monitor. Hence, understanding the emissions in highly congested traffic is essential to understanding why roadside air quality monitors are consistently exceeding European air quality guidelines. The emissions during the higher speed driving on the WLTC and RDE are largely irrelevant to addressing the issue of poor local air quality.

In a vehicle with no energy storage the energy used to accelerate the vehicle from stationary is thrown away when the vehicle stops. In congested traffic these stop/start events occur very frequently and are shown in this work to result in very high fuel consumption and CO_2 emissions. Related to the number of accelerations from idle is the proportion of the journey time that is spent at idle in slowly moving traffic. Table 1 shows that this was much higher in the congested traffic work of Khalfan [17] than for any of the test cycles and that the proposed RDE has practically no time at idle after the first vehicle start. This low speed stop/start congested traffic movement is an area where energy storage using regenerative braking, as in hybrid vehicles, can be effective in reducing overall fuel consumption. Thus hybrid vehicles will be most effective in congested traffic and least effective in freely moving traffic, as the extra weight of batteries and motors increase the fuel consumption. This is likely to result in a relatively poor performance of hybrid vehicles on the RDE test cycles. Also, where the proportion of time at idle is high, as in congested traffic, the benefits of engine automatic switch off at idle are greater and this technology is coming into most passenger car vehicles, not just hybrid vehicles.

Table 1 shows that the key differences between the WLTC and RDE legislation and the existing NEDC, FTP and JC09 are the higher average speeds and the complete lack of congested driving, with reduced number of stop/starts. The longer distances of the cycles means that the cold start portion, which lasts about 1km [16], is a lower proportion of the whole cycle. This means that the cold start emissions are divided by a longer distance to produce apparently lower emissions, but actually the same emissions over the first km. The WLTC has a higher mean velocity than the NEDC or FTP, double the test distance and a quarter of the number of starts from idle. All this leads to lower emissions than the NEDC [21], as shown by Williams et al. [22] for Euro 6 vehicles.

Liu et al. [23] analysed data for USA vehicle trips with 1851 trips using 292 passenger car vehicles driving a total of 25,000km. 50% of the trips were <4km, 25% were 4-8km and only 25% were for distances >8km. This justifies the use of a 5km trip distance in the previous work of the authors [13, 15-17] and in this work. The trip analysis of Liu et al. [23] also shows the unrealistic trip distance in RDE test procedures, as <1% of journeys were of this length.

The RDE test procedures are weighted to higher vehicle speeds using higher engine powers, where for SI engines the catalyst will always be hot and lambda 1 control is precise. This results in SI engine vehicles always meeting the NEDC legislation under RDE conditions. However, it will be shown in this work that under low speed congested traffic conditions emissions can be well above the NEDC values.

The objective of this work is to further analyze the real world emissions data of Khalfan et al. [17] by splitting the 5km journey into 10 sections of between 0.24 and 0.74km, which coincide with specific road features such as traffic lights and road junctions. The 29 repeated journeys then give 29 measured emissions for each of the 10 sections, 290 measurements in total. This will enable the most congested traffic part of the journey to be assessed for emissions. It will be shown that the most congested sections of the 5km journey dominate the total emissions for the journey.

Experimental Methods

A Euro4 emission compliant Ford Mondeo manual transmission petrol car was used, which was fitted with a port fuel injected 1.8 litre 16V spark ignition engine with 4 cylinders and 16 valves. The odometer reading on the car was 7,100 km prior to the tests. The vehicle was equipped with a Three Way Catalyst (TWC). The curb weight of the car was 1374 kg. The car was instrumented with 3 thermocouples, which measured the lubricating oil in sump temperature and the exhaust gas temperatures upstream and downstream of the TWC. All temperatures were measured using grounded junction mineral insulated Type K thermocouples, with a response time of ~0.25s.

The present results are for a manual transmission vehicle and driving in a non-optimum gear is one real world effect that is specific to manual transmission vehicles. However, in congested traffic the vehicle motion is primarily controlled by the action of other traffic and is not in the free choice of the driver. Under these circumstances there is less difference between manual and automatic transmission. It is on more freely moving traffic at higher average speeds, such as in the RDE and WLTC test cycles, that the gear ratio used is controlled by the driver and not by the other traffic. Under these circumstances real world driving would result in differences between emissions and fuel consumption between manual and automatic transmissions.

The manual transmission used in the present work would be unusual for real world driving in the USA, where 96% of passenger cars had automatic transmission in 2016 [24]. In the USA automatic transmissions have been >90% of passenger cars since 2000. However, this is not true of the rest of the world and the global average is 68% manual transmission estimated for 2017 [24] and in Europe manual transmissions are 82% of the market [25]. So real world emissions for manual transmission cars is more relevant to congested city driving on a global basis, but not for the USA. In stop/start congested traffic driving where most of the motion is in first gear, the benefits of automatic transmissions are reduced. There are no advantages of automatic transmissions in fuel consumption or CO_2 emissions and most evidence is that there is a small increase in fuel consumption. Thus, the present evidence for real world emissions in congested traffic using a manual transmission car is most applicable for driving outside the USA, but will not be much different for USA congested traffic with automatic transmission vehicles.

The present work was carried out in a Euro 4 vehicle with a hot start, the differences in emissions for a Euro 6 SI vehicle, excluding the cold start are small. It will be shown that the present vehicle meets Euro 6 emissions regulations for NO_x for average speeds above 25 kph and that NO_x exceedances were due to the types of stop/start traffic movement in congested low speed traffic. The CO and UHC emissions for Euro 4, 5 and 6 are the same, so the high CO and UHC emissions found in this work in congested traffic are not strongly influenced by the emissions control technology.

A Racelogic VBOX II differential GPS system was used to provide geographical position, speed and acceleration data. The VBOX II is a GPS data logging system developed by Racelogic specifically for automotive applications. It is normally used for race track testing and other performance testing where accurate speed, position and acceleration data is required for driver performance evaluation. Data was logged at 1 Hz and stored on to a compact flash memory card, and subsequently transferred to a PC. The analogue output from the VBOX II was a 0-5V DC signal corresponding to road speed, and was fed to the data logger and then a laptop.

A MAX710 fuel flow measurement system was connected between the fuel tank and engine. This measured the fuel mass flow rate using a level controlled recirculation tank, transfer pump and a high-resolution flow meter. The pump maintained a constant pressure to the recirculation tank that fed fuel to the engine. This recirculation tank collected return fuel from the engine and recirculated this fuel back to the engine instead of returning it to the fuel tank. This recirculation loop allowed the use of a single meter to measure make-up fuel as it replaced the fuel consumed by the engine. Total fuel consumption was determined to better than 1% accuracy. The rate of fuel consumption was determined with a 1-second resolution. Standard ultra-low sulfur RON95 petrol fuel was used throughout the tests.

The air/fuel ratio was measured using a Horiba “Lambda Checker LD-700” in terms of lambda with a response time of 0.08 ~ 0.15 second. The lambda sensor was mounted downstream of the catalyst and upstream of the tailpipe Horiba pitot tube mass flow measurement system. The LD-700 used an NGK wide band oxygen sensor (ZrO_2 type). The unit was calibrated for a fuel with a hydrogen/carbon ratio of 1.85 and an oxygen/carbon ratio of 0. The accuracy of the unit was ± 0.04λ for 0.91~1.19 λ and ± 0.08 λ outside this range. The LD-700 had a DC output of 0-5 volts, which was directly proportional to lambda. The DC voltage output was logged into a data logger and then into a laptop.

The gas sample was taken downstream of the catalyst at the tailpipe using the Horiba pitot tube exhaust mass flow measurement system and associated mean exhaust gas sampling system [26, 27]. The heated sample line was passed through a small hole in the car’s floor pan. The exhaust mass flow measurement and the gas sample were time aligned as they were sampled from the same location. The lambda probe then enabled the air mass flow to be calculated from the exhaust mass flow and the air/fuel ratio determined by the lambda probe. The time difference between the lambda probe and the exhaust mass flow was small as they were about 0.3m apart. The Horiba pitot static exhaust mass flow measurement system had an exhaust extension added that prevented flow pulsations from entraining air back into the exhaust where sample dilution could occur. This was a problem at idle without the exhaust extension [26, 27].

The fuel flow could also be derived from the measured exhaust mass flow rate (which is the air plus fuel mass flow, A + F) and the lambda probe A/F determination by Eq. 2.

$$\text{Fuel flow rate, } F = (A + F) / (1 + A/F) \qquad (2)$$

This was used in the data analysis as there was then time alignment between the emissions measurement, the exhaust mass flow and the fuel flow that gave rise to the measured exhaust composition. If the MAX 710 fuel flow meter was used in the data processing there would be a time alignment problem as the fuel flow was measured at the inlet to the engine and the exhaust composition at the outlet. This would then result in incorrect conversion to mass emissions as a function of time. The MAX710 fuel flow meter was used primarily to accurately determine the total fuel flow rate over the whole journey, as the time alignment was then not important. If the time difference between the input and exhaust was say 1s then in a 1000s journey this would be a negligible error in total fuel consumption. However, for the second by second resolution of the emissions during an acceleration the conversion to mass could suffer from time alignment problems using the MAX710 fuel flow meter. This is why all the measurements were made close to the exhaust tailpipe so as to minimize time differences in the various measurements.

A portable Fourier Transform Infrared (FTIR) spectrometer was used to measure on road real world emissions. The model used was the Temet Gasmet CR 2000 which had liquid nitrogen detector cooling and was capable of measuring concentrations as low as 0.5~3 ppm, depending on the species. It was specifically calibrated by the manufacturer to an accuracy of 2% within the calibrated measurement range; which was 20 - 9960 ppm for CO (26 point calibration), 0.3 - 30% for CO_2 (10 point calibration) and 20 -10,000 ppm for NOx (36 point calibration) respectively.

A FTIR emission measurement system was selected because of its ability to speciate VOC, $NO/NO_2/N_2O$ and measure ammonia in addition to CO, NOx, and THC emissions. The FTIR measurement for regulated emissions was calibrated against standard CVS measurements using engine dynamometer testing [26] and a chassis dynamometer test facility over various driving cycles [27]. It was found that the FTIR measurements had excellent agreement (2% deviation) with the CVS measurement for CO_2 emissions. The Temet instrument comprised a FTIR analyzer, a portable sample handling unit (filtering and controlling sample flow), heated sample lines and a laptop. The system weighed approximately 30 kg. The entire on-board measurement instrumentation including the FTIR system, the fuel consumption measurement system, two batteries and a DC-AC converter weighed 150 kg. This was equivalent to a second person in the car and in the tests there was only the driver in the car. Thus the overall vehicle weight was representative of real vehicle driving with two person occupancy.

The time alignment between the FTIR and the exhaust flow rate used the voltage output from the VBox and the throttle movement sensor as external signals to reference the time of events on the road. There were two laptops for data logging and processing: one for the FTIR that logged emission spectra and the external time alignment signals; the other one was for temperature and fuel meter logging. This FTIR output time alignment was necessary to account for the sample time from the exhaust sample point to the FTIR detection chamber.

The power needed for the on-board measuring system was around 1.2 kWs and this would have necessitated drawing up to 100 A at 12V from the car's electrical system. This would have required an upgraded alternator and increased the load on the engine, therefore affecting the emissions characteristics. Another possibility was to use a small dedicated generator but this option is only feasible in large heavy duty vehicles. Therefore, a dedicated power supply, two 12V battery packs and an on-board DC-AC converter, were used to provide 240V AC necessary for instrument operation. The two batteries used weighed a total of 70 kg. They provided approximately 2-3 hours of operation before needing recharging.

In order to measure wet concentrations, the raw undiluted sample gas extracted from the exhaust system was maintained at about 180℃ to prevent low boiling point pollutants being lost due to condensation. The extracted exhaust sample was hot filtered, so that the sample cell remained free of particulates which would contaminate it and shorten its lifetime. The sample handling unit used a heated pump to continuously extract a gas sample from the vehicle's exhaust system at a constant flow rate (2~3 l/min) via a heated line. This was then hot filtered using a 0.2 µm filter and introduced via another heated line into the sample cell of the FTIR. Both heated lines were maintained to 180℃ by the sample handling unit. The sample handling unit consumed the most power since it performed heating and pumping functions. It was installed in the boot of the car along with the FTIR.

Mass Emission

The FTIR emission measurements were on a volumetric basis. These were converted into a mass basis using the conventional method for the computation of emissions index (EI, g/kg fuel) as in Eq. 3.

$$EI = 1000{*}K{*}C{*}(1+A/F) \text{ g/kg fuel} \qquad (3)$$

Where

- K is conversion coefficient, which is the ratio of molecular weight of a certain emission component to the molecular weight of the whole sample gas. The molecular weight of the exhaust sample gas is close to that of air and does not vary more than 1% for H/C ratios of about 2 (i.e. gasoline), irrespective of the air/fuel ratio. For this reason, K is here treated as a constant.
- C is the concentration of the component. If this is measured in ppm or % then the equation has to be multiplied by 10^{-6} or 10^{-2} respectively.

- A/F is the air/fuel ratio on a mass basis measured by the lambda sensor.

The EI was then converted into mass emission rate g/s using fuel consumption measured for the sampling period. Then the distance based emissions can be calculated for any distance traveled.

Vehicle Specific Power, VSP - W/kg or kW/tonne

VSP is defined as the instantaneous power per unit mass of the vehicle, with units of kW/tonne or W/kg. The VSP essentially measures the brake power output of the engine and this together with the fuel consumption enables the engine thermal efficiency to be determined as power out / fuel thermal power in. Also, the cumulative power in kWh can be determined from the VSP measurements. This VSP determination from the GPS data is the basis of the power binning method in RDE emissions evaluation [18-20].

The VSP estimation equation that was used was that in Eq. 4 with the coefficient values for a light-duty vehicle [28-30].

$$VSP=v*(1.1*a+9.81*\sin(\mathrm{atan}(grade))+0.132)+0.000302*(v)^3 \quad (4)$$

where:

- v is vehicle speed (m/s)
- a is vehicle acceleration (m/s^2)
- grade is road grade, = vertical rise/horizontal distance (dimensionless)

For zero gradient and no aerodynamic drag term (v^3) Eq. 3 reverts to the commonly used VSP as the product of va m^2/s^3, which may be shown to be the same units as W/kg. VSP is calculated in the present work so that the real world engine power demand can be determined. The present vehicle weight was 1.37 tonnes and the engine power output in kW can thus be determined, which combined with the fuel flow rate and its calorific value enables the thermal efficiency to be determined.

Congested Traffic in Urban Areas

The legal speed for the road investigated in this paper is 48 km/h. The average speed on the NEDC is 33.6 km/h and this is an average CF of 30%. For the urban part only of the NEDC the average speed is 17.2 km/h and congestion is 64% which is more reasonable. However, in this work CF up to 90% have been measured and 95% in the worst congested parts of the route. The new WLTP is little improvement on the NEDC as the average speed is higher so the congestion is lower, which is the main reason why it has been found to give lower emissions than on the NEDC for many vehicles [21, 22].

Features of congested roads:

1. A high traffic flow in vehicles per hour per lane
2. Frequent junctions on the route with traffic joining and leaving the main flow. Main flow stops to let in vehicles from the right or left, at the discretion of the drivers in the main flow. Each car joining causes the main traffic to halt.
3. Traffic lights at major junctions and pedestrian crossings. All traffic now halts periodically. For high traffic flows it can take several stop/starts to get through. The process of starting and moving about 10m is very energy intensive with high emissions.
4. Traffic joining and leaving flows that can be comparable with the main flow.
5. Traffic mean velocity decreases as congestion increases.
6. The number of stop/starts increase as congestion increases.
7. The proportion of time at idle increases as congestion increases

Test Route and Procedures

The emissions from the instrumented vehicle in the traffic were studied on a major radial road into Leeds city centre. The most congested part of this route was used where the road passed through the suburb of Headingley, where a roadside air quality monitoring station was based. The route is shown in Fig.1; the distance of each trip was 5 km. The speed limit on these urban streets is 48 km/h (30 mph) and an uncongested traffic flow would have an average speed close to 48 km/h. Two different cycles were conducted as summarized in Table 2. The two routes had different numbers of right and left turns: 8 right and 3 left for route A and 5 right and 6 left in route B. There were 3 sets of traffic lights and 4 pedestrian crossings on the route and these give rise to many stop/start events on each journey, but for some journeys they were all green. For the twenty nine individual vehicle journeys, the speed was controlled by the vehicle in front and not by the driver.

Figure 1. Map and notations of the driving route.

Table 2. Directions of the two driving routes

Driving cycle (route)	Direction
A	1-2-3-4
B	1-3-2-4

Figure 2. Map of sections of the journey in Table 3.

Table 3. 10 journey sections for locations in Fig. 2

A journey					
Section	**Section start**	**Section end**	**same section**	**Section**	**Distance km**
S1	1	3	**S1=S10**	**S1**	**0.719**
S2	3	4	**S2=S9**	**S2**	**0.24**
S3	4	6	**S3=S6**	**S3**	**0.289**
S4	6	8	**S4=S5**	**S4**	**0.535**
S5	8	9	**S7=S8**	**S5**	**0.684**
S6	9	11		**S6**	**0.244**
S7	11	15		**S7**	**0.662**
S8	15	19		**S8**	**0.586**
S9	19	20		**S9**	**0.202**
S10	20	22		**S10**	**0.739**

The city of Leeds data showed that at an average speed of 10 kph the average distance per vehicle was 10m and at 20 kph it was 50m [17]. For higher speeds than 20 kph the individual vehicle speed was more controlled by the driver than the other traffic as the distance apart of the vehicles was >50m. The journeys were undertaken at different times of the day and on different days over several weeks, so as to experience a wide range of traffic congestion conditions. These journeys are typical of congested city traffic in many UK and European cities and are typical of the urban driving close to roadside air quality monitors.

The traffic flows on this road were measured by Leeds City Council [12-14]. The distance they used on this road was 3.5km and the time of a vehicle in the flow to travel this distance at different times of the day was measured. These travel time results were analysed by Khalfan et al. [17] to determine the mean velocity and CF as a function of the traffic flow in vehicles per hour, vph. The section of road that Leeds City Council used included points 2 – 7 in Fig. 2 and hence the mean velocities measured in the present work can be used to convert to traffic densities using the Leeds City Council data as was done by Khalfan et al. [17]. This showed that as the number of vehicles per lane per hour (traffic flow or traffic density) increased the mean speed decreased and the congestion increased. Also the average distance between vehicles decreased as the traffic flow increased, until the vehicle in front does not control the individual speeds and accelerations, but does control the average speed.

The peak traffic flow or load was 1000 vehicles/hour/lane [12-14], but the road was a single traffic lane in each direction with a cycle lane alongside. In the USA and in China, 2 – 4 lane roads in each direction pass into the centre of many large cities and the total traffic loads are higher than in Leeds before they are congested. To achieve the present level of congestion in a four line highway the vehicle flow would be about 4000 vehicles per hour. The impact on the local air quality would be greater, as shown in many Chinese cities today. However, the emissions per vehicle would be similar to that in the present work.

This work splits these journeys into 10 sections and analyses the mean emissions for each section. This enabled the most congested portion of the 5km route to be identified and the range of mean velocities in the previous work [17] to be extended. The key points in the 5km loop journey in Fig. 1 are shown in Fig. 2 and the sections of the journey are summarized in Table 3, which are the same sections for journey A and B.

Table 3 shows that there are five sections on the journey, but travelled in the opposite direction on the return journey, where different traffic flows and different actions at traffic lights and pedestrian crossings occur. Thus the return journeys have been treated as a separate journey and the results are presented for the 10 sections of the route. The Headingley roadside air quality monitor is between points 19 and 20 in Fig. 2 and hence S2 and S9 are the two parts of the journey that pass the roadside monitor. The data for S2 and S9 will be presented later to show the high emissions local to the monitor. The 10 sections of the journey in Table 3 can be seen in terms of velocity and acceleration in Figs. 3 and 4, for high and low congestion respectively. For each of these sections the 29 repeat journeys have been separated into 10 sections giving 290 data points for average fuel consumption and emissions for each section.

Results

The Number of Stop/Starts

Examples of the instantaneous emissions have been published by the authors for cold [16] and hot starts [17] and will not be repeated here. This paper includes a more detailed analysis of the hot start data than the for the mean journey emissions [17]. Several of the detailed vehicle velocity, acceleration and emissions v. time plots have been given in the previous publications [16, 17] and will not be repeated here, apart from those in Figs. 3 and 4 that explain the sections of the journeys that were analysed in this work.

Fig.5 shows the number of starts from idle (<5 km/h) for the 29 hot start and 8 cold start 5km journeys [13]. This shows that low average speeds are associated with a high number of stop/starts in journeys with high congestion and low mean

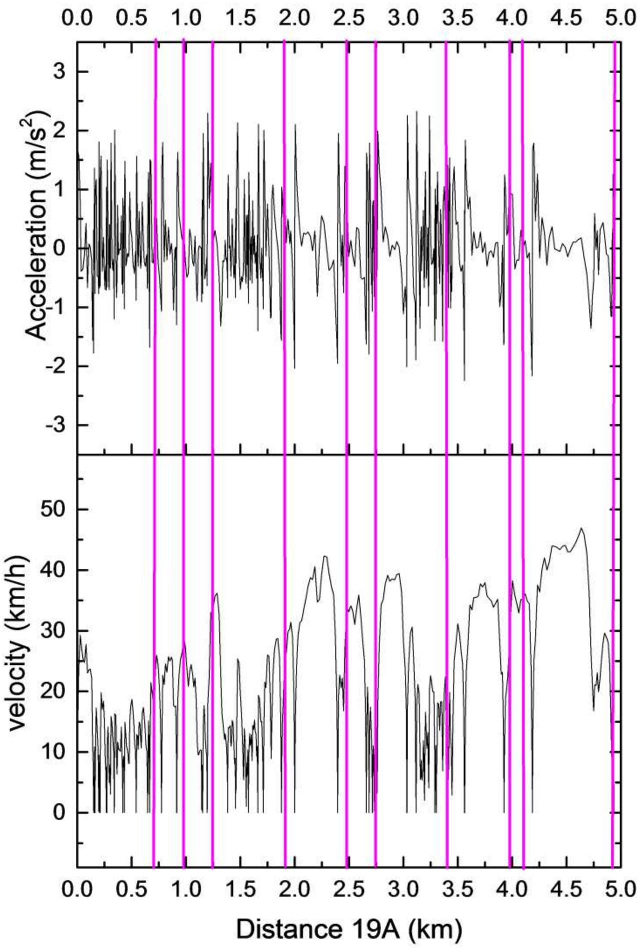

Figure 3. Velocity and acceleration records for high congestion (6 stop/starts per km) as a function of distance showing the 10 stages in Table 3

Velocities in Fig. 5 also shows the number of stop/starts in the various test cycles in Table 1 and this shows that none of these test cycles includes the traffic conditions involved in congested traffic in cities, with large numbers of stop/starts per km. The WLTC, which is supposed to be more real world than the NEDC, has fewer stop/starts and a higher average speed and hence is not representative at all of congested traffic driving. As a consequence data from WLTC tests and NEDC tests on the same vehicles show lower emissions and lower CO_2 for the WLTC [21, 22]. Thus the WLTC is not going to give data that explains why air quality in cities is not improving in proportion to the improvement in vehicle emissions. This will only come from studying the congested traffic in the vicinity of the air quality monitoring stations in cities, as in the present work.

Hybrid vehicles are particularly suitable to stop/start congested traffic conditions, as most of the starts will use stored energy and not fuel burnt in an engine. The benefit of hybrid vehicles in congested traffic will depend on the state of charge, SOC, of the batteries. For plug in hybrids it is more likely that the

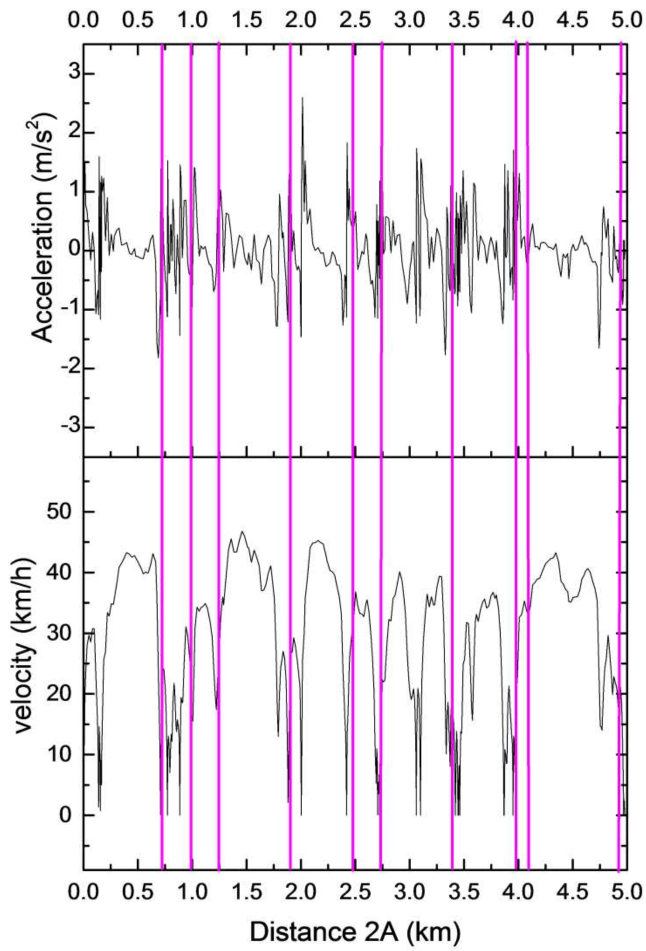

Figure 4. Velocity and acceleration records for low congestion (2.4 stop/starts per km) as a function of distance showing the 10 stages in Table 3

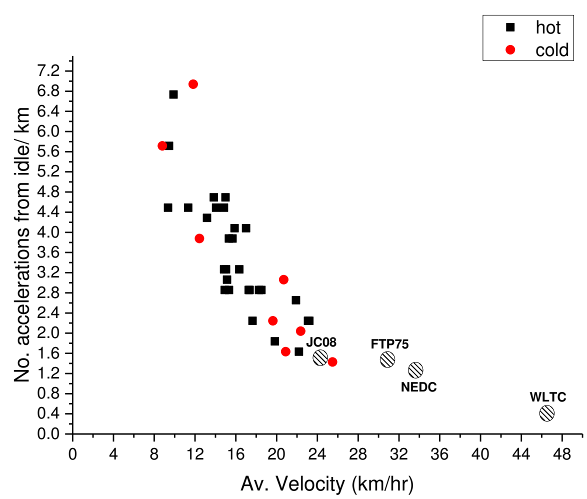

Figure 5. Number of accelerations from idle vs mean trip velocity for cold and hot start trips

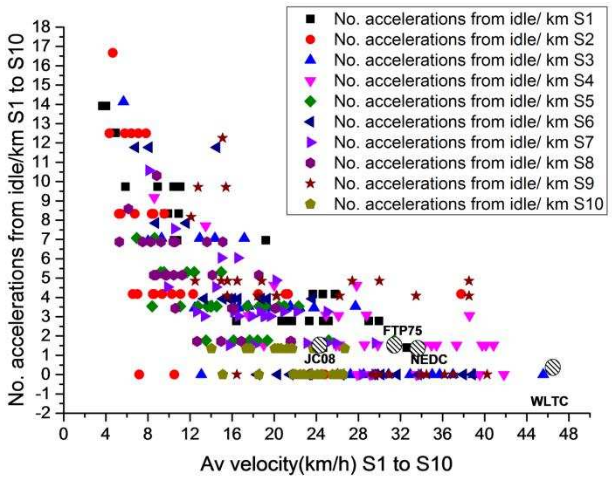

Figure 6. Number of accelerations from idle (<5km/h) per km for the 10 journey sections in Table 3.

batteries will be fully charged for the morning commute to work, when congested traffic is most likely to be met. Conversely, hybrid vehicles will have little benefit on the WLTC as there are few stop/starts and high average speeds. The vehicle's SI or diesel engine works efficiently at high powers, so the benefit of the electric drive in comparison is lower. If representative stop/starts for congested traffic are not in the test cycles for passenger car vehicles then there is little incentive to develop hybrid technologies. The omission of cold start and stop/start congested traffic from RDE test cycles means that Hybrid vehicles will be disadvantaged relative to non-hybrids on the RDE journeys.

Figure 6 shows the number of stop/starts per km as a function of the mean velocity of each stage, for the 10 journey sections with 29 hot start journeys in each (290 data points). Fig. 6 shows a wider range of mean velocities from 4 to 46 km/h, instead of 8.5 – 25 km/h in Fig. 5. At the higher mean velocities the number of stop/starts reduces to those in the test cycles, one journey section having conditions close to the WLTC in terms of the mean velocity and the zero stop/starts per km. This occurs on section S4 which is directly after a set of lights. In low congestion when the lights are on red the road ahead will be clear and once on green the front traffic can accelerate away with no influence of other traffic. This resulted in near WLTC conditions in this local region. However, this was a rare occurrence as shown in Fig. 6, as normally when the traffic lights were on red traffic would move from the left and right roads at the junction to fill up the road ahead so that when the traffic lights turned green the road ahead was not empty and hence the traffic movement was controlled by the other traffic.

Fig. 6 also shows that the number of stop/starts per km had a greater range from 0 – 17, compared with 1.3 – 7 in Fig. 5. Twenty one of the 290 journeys had a number of stop/starts >10 per km or one stop/start every 100m on average. This is mainly caused by queuing at traffic lights in congested traffic. At 5 km/h a 100m distance takes 139s and this is similar to the green on time at traffic lights. On the tested route the traffic lights are computer controlled to maximize the traffic flow in the direction into the city centre in the morning and out of the city centre in the afternoon, so that the green on period is variable.

Fig. 6 shows the general trend of Fig. 5, that higher average speeds is accompanied by few stop/starts. However, at low mean velocities, such as 8 km/h, the number of stop/starts varies from 0 to 12/km for journey 2 in Table 3. This is the section that leads up to a set of traffic lights. In contrast section 1 has a number of stop/starts per km that increase as the mean velocity decreases. The reason for this difference in two connected sections of the journey is that in times of high congestion the traffic queue backs up to SI and there is a large number of stop/start movements, as shown in Fig. 3. However, S2 can move slowly or quickly depending on whether the lights are on green. Fig. 3 shows that S2 has a relatively high velocity, compared with the stop/start traffic in S1 for the same journey.

Fig. 4 shows the reverse situation for low congestion with relatively free moving traffic in S1 and stop/start traffic in S2. Fig. 6 shows that the section of the journey S3 also had a wide range of stop/starts per km and this was again due to this section have a second set of traffic lights at the road junction at the end of this section and a pedestrian crossing in the middle of the section. This S3 section of the journey has mean velocities from 13 to 46 km/h with no stop/starts. These are all journeys with green traffic lights at the end of S3 and the velocity decreases as the traffic load increases. The higher number of stop/starts in S3 occur when the traffic lights are on red for part of the time and the mean velocity is low.

Thermal Efficiency in Congested Traffic

The VSP data from Eq. 4 was used to determine the total MJ power output for each section of the journey, for all 29 journeys. The fuel flow rate data was used to determine the total fuel consumed during each section of the journey and this was converted to MJ of input energy using a fuel CV of 43 MJ/kg. This enabled the average thermal efficiency for each section of the journey to be determined and this is shown in Fig. 7 as a function of the mean velocity for each section. The results in Fig. 7 show a very wide data scatter, which was due to the influence of the proportion of idle. Idle has no power output, but does consume fuel and has emissions. So the impact of idle is to reduce the thermal efficiency and to reduce the mean journey speed.

Comparison of Figs. 7 and 6 shows that at the lowest thermal efficiency of 8% at 4 km/h there were 14 starts from idle per km and the proportion of time at idle in this journey would be high. In contrast there was a journey at 10 km/h that had a thermal efficiency of 23% because there were no starts from idle and hence no idle period in the journey. In contrast a journey with an average velocity of 9 km/h had a thermal efficiency of 9.5% because it had 12.5 starts from idle per km. Thus it is not the low average velocity that causes low thermal efficiencies and high CO_2 but the frequency of the stop/starts per km.

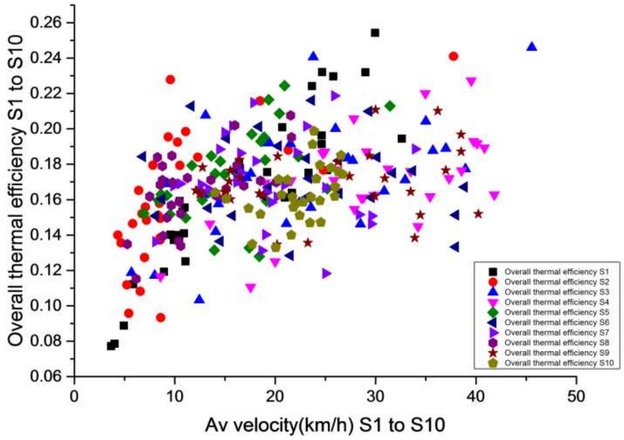

Figure 7. The average thermal efficiency for each journey section as a function of the average velocity.

These real world congested traffic thermal efficiencies are similar to those measured for US vehicles of model year 2015 over the FTP75 test cycle [31, 32]. Reiss analysed the propulsion efficiency of vehicles (thermal efficiency in this work) as a function of the average power as a proportion of the rated power of the engine [31, 32]. For 1% of maximum power the thermal efficiency was 10%, for 2% it was 12-18%, at 3% it was 15 – 20% and at 5% it was 18 – 25% depending on the vehicle under test. These results are very close to the present measurements in Fig. 7 with 10% thermal efficiency at a journey average speed of 5 kph (about 1% power) and 14 – 26% at 30 kph (about 5% power). For hybrid vehicles Reiss found efficiencies of 22 – 28% at 3% power and 25 – 31% at 5% power. This shows that the largest efficiency improvement for hybrid vehicles is at the lowest engine powers or vehicle speeds. This is because the stop/start vehicle motion occurs at these low powers, where hybrid engines have the greatest benefit.

The Exhaust Temperatures Upstream and Downstream of the TWC

The tests were carried out with a prior journey to warm up the engine lube oil, coolant and TWC. Typical results for the exhaust temperature 25mm upstream of the catalyst front face and 25mm downstream of the catalyst rear face temperatures and the associated vehicle acceleration are shown in Fig. 8 for a stop/start congested traffic journey and in Fig. 9 for a less congested journey. The less congested journey had fewer accelerations from idle and this used less fuel and lower powers. This resulted in the exhaust temperature upstream of the catalyst being lower in Fig. 9 than in Fig. 8 for higher congestion. The thermal inertia of the TWC substrate makes the outlet temperature much more uniform than the inlet temperature.

The downstream temperature was 350°C at the beginning of the hot start, as shown in Figs. 8 and 9, due to the residual heat in the catalyst with good thermal insulation. The catalyst downstream temperature was above 400°C within 10s for both

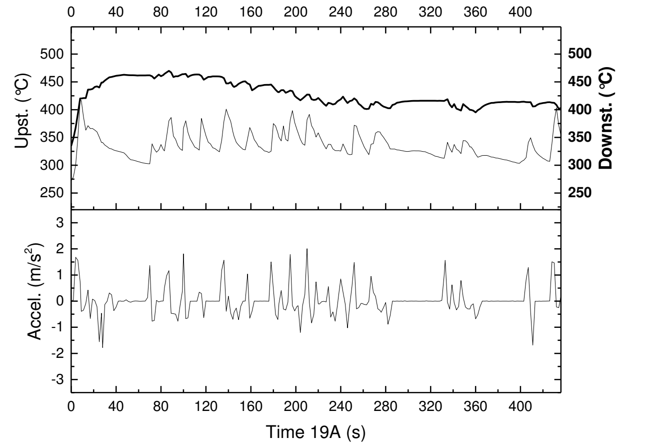

Figure 8. TWC front face and rear face temperature for highly congested traffic

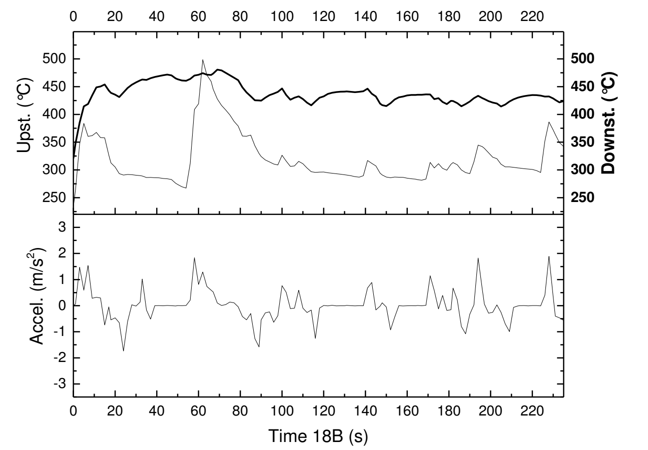

Figure 9. TWC front and rear face temperature for lower congestion then in Fig. 8.

levels of congestion. This heating was due to the chemical heat release through oxidation of engine out HC and CO which heated the exhaust gases passing through the catalyst. Typically around 5% of the energy in the fuel is released at the catalyst in a SI engine under low power conditions and this is the prime heating mode for the catalyst in the present work. The upstream temperature varied with acceleration, as this is controlled by the engine power demand and the exhaust temperature increases with power. The initial acceleration occurred in a side road with no congestion and once the main traffic flow was joined the idle periods had low exhaust manifold outlet temperatures. However, the heat release from the HC and CO oxidation kept the TWC outlet temperature high.

It will be shown that the journey S1, which includes the hot start, had higher emissions than all the other journeys. This was due to the lower inlet temperatures to the catalyst shown in Figs. 8 and 9. By the end of section S1 the upstream and downstream temperatures were above 400°C, as shown in Figs. 8 and 9 after 450s. Figures 8 and 9 show that the

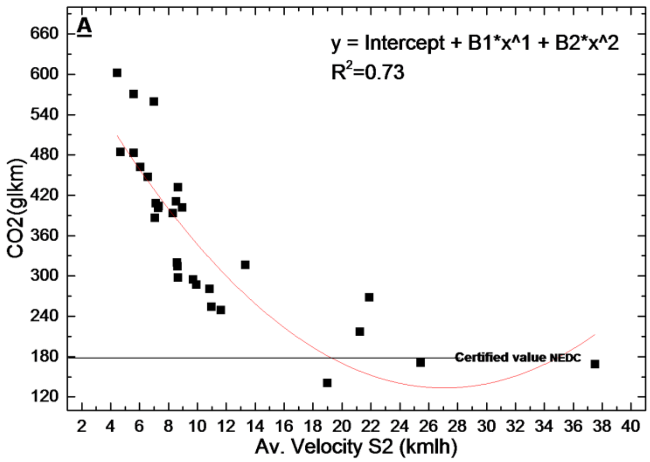

Figure 10. CO_2 emissions for S2 v. the mean velocity for S2

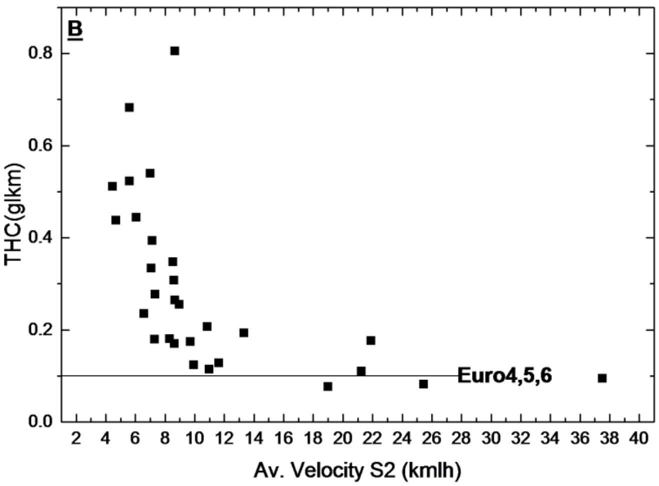

Figure 11. THC emissions for S2 v. the mean velocity for S2

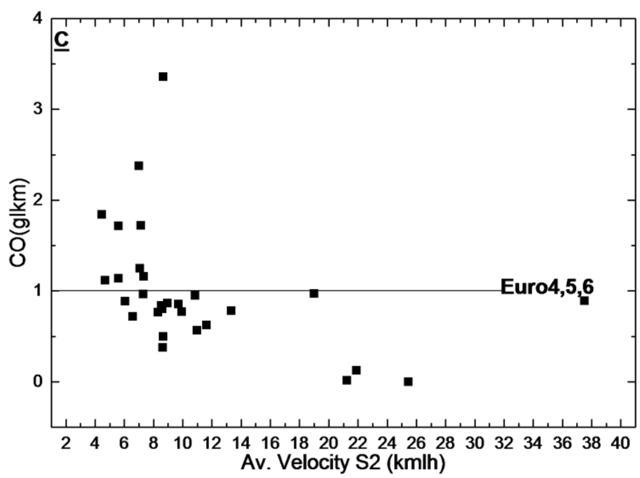

Figure 12. CO emissions for S2 v. the mean velocity for S2

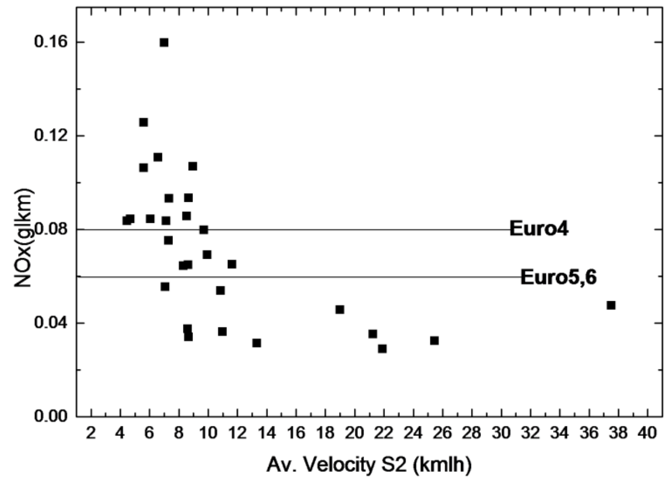

Figure 13. NO_x emissions for S2 v. the mean velocity for S2

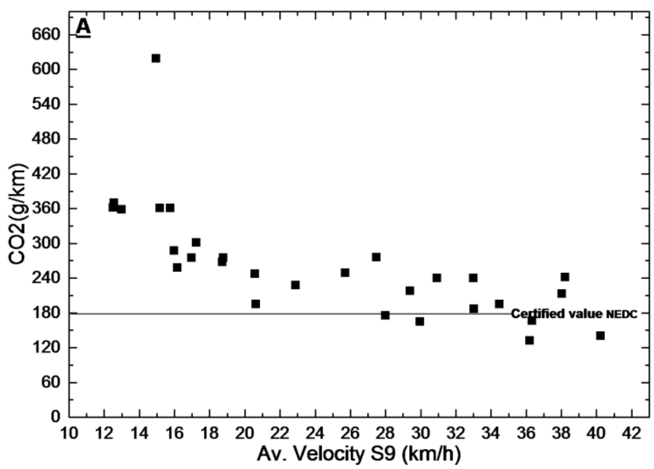

Figure 14. CO_2 emissions for S9 v. the mean velocity for S9

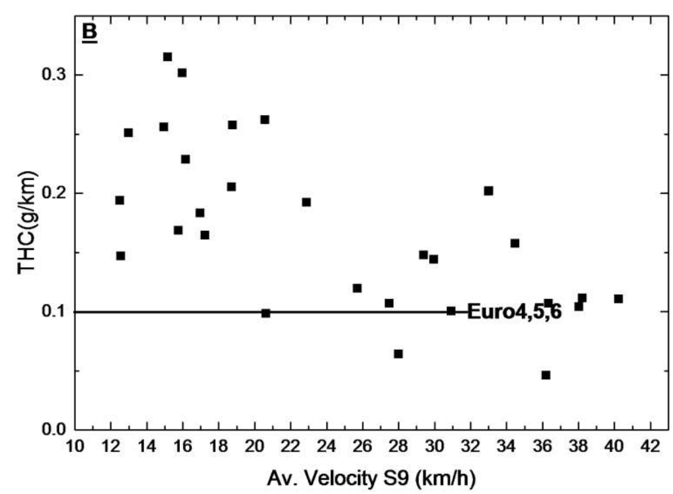

Figure 15. THC emissions for S9 v. the mean velocity for S9

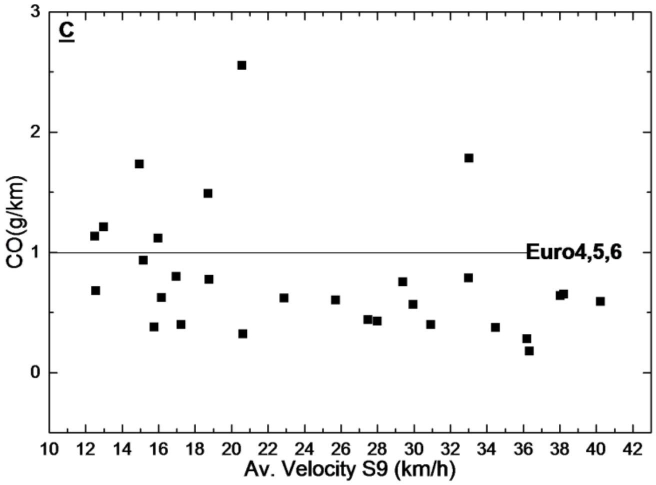

Figure 16. CO emissions for S9 v. the mean velocity for S9

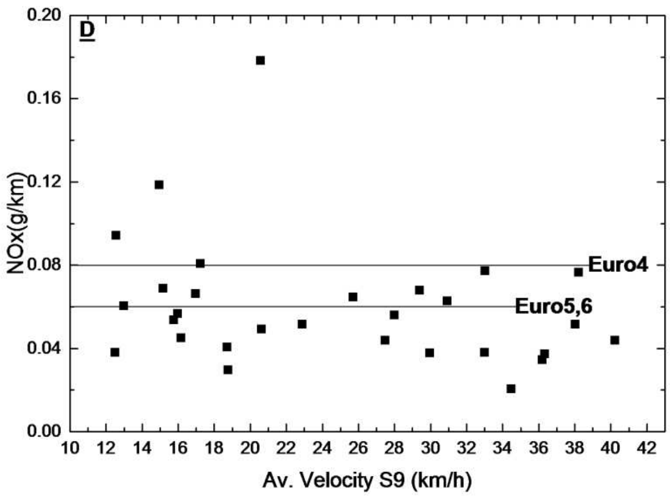

Figure 17. NO_x emissions for S9 v. the mean velocity for S9

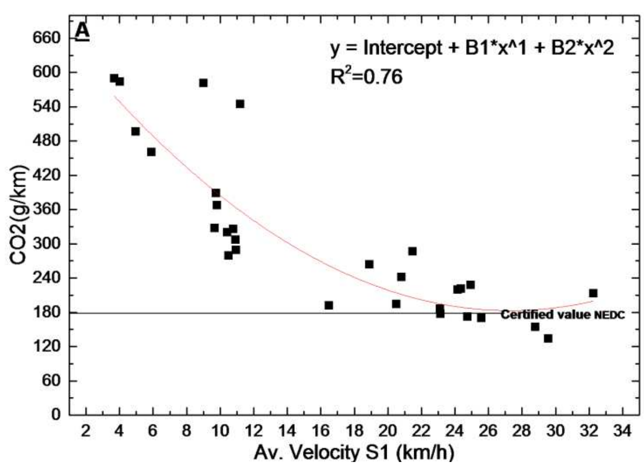

Figure 18. CO_2 emissions for S1 v. the mean velocity for S1

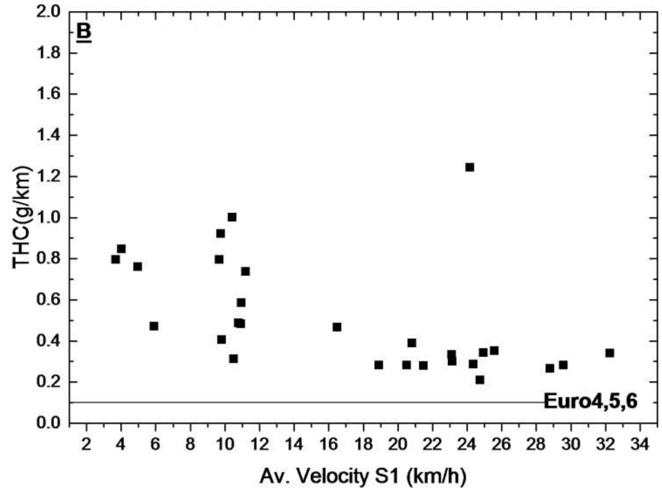

Figure 19. THC emissions for S1 v. the mean velocity for S1

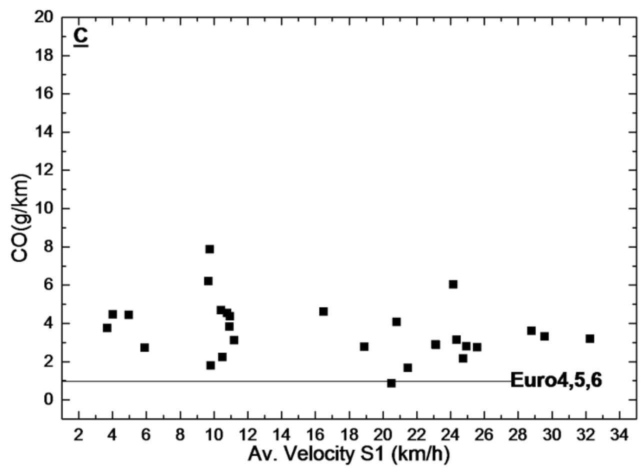

Figure 20. CO emissions for S1 v. the mean velocity for S1

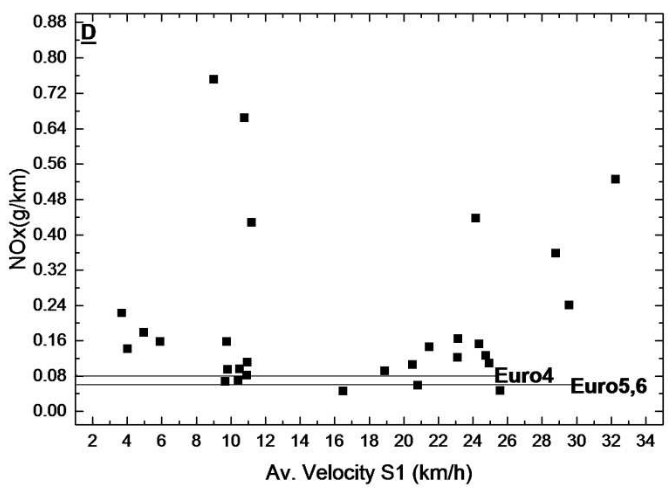

Figure 21. NO_x emissions for S1 v. the mean velocity for S1

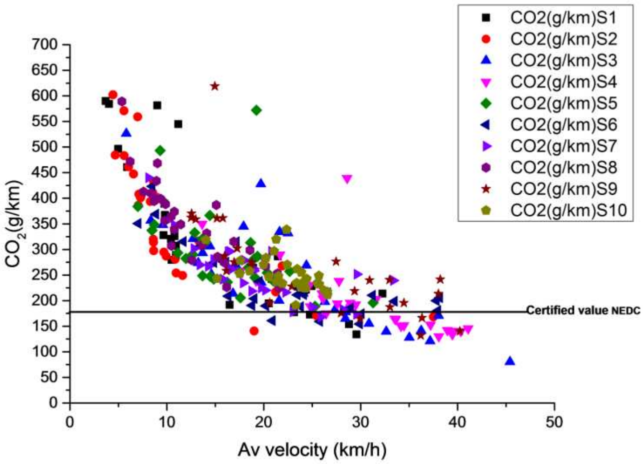

Figure 22. CO_2 emissions for S1-S10 v. the mean velocity

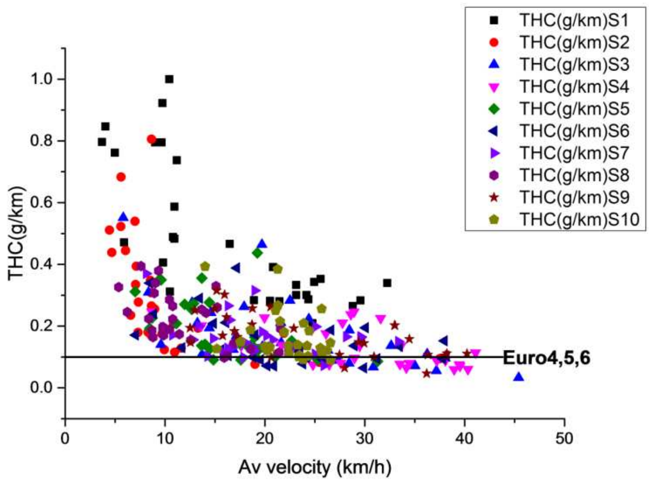

Figure 23. THC emissions for S1 – S10 v. the mean velocity

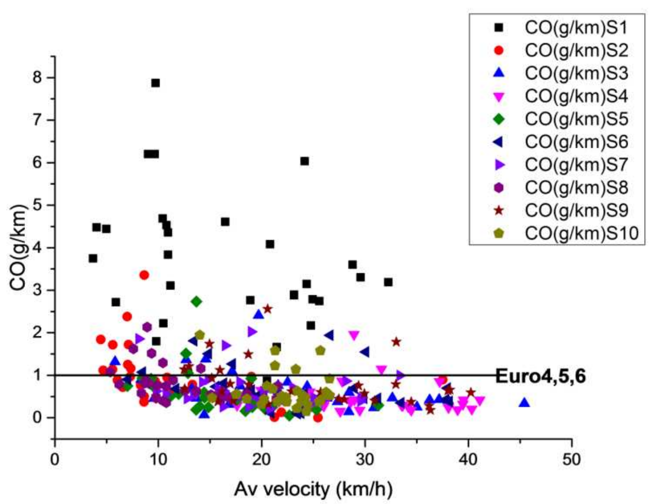

Figure 24. CO emissions for S1-S10 v. the mean velocity

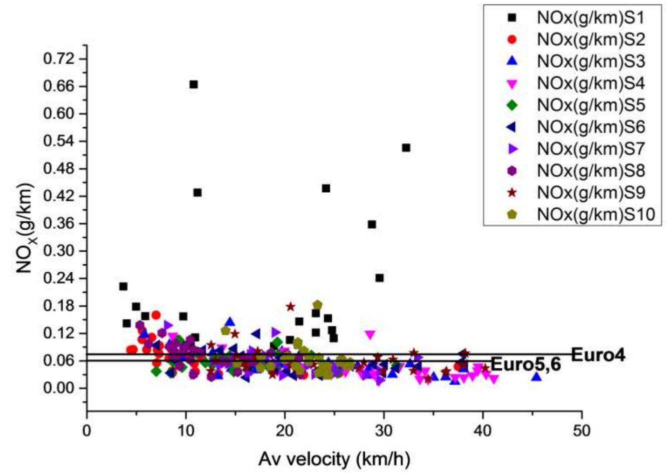

Figure 25. NO_x emissions for S1 – S10 v. the mean velocity

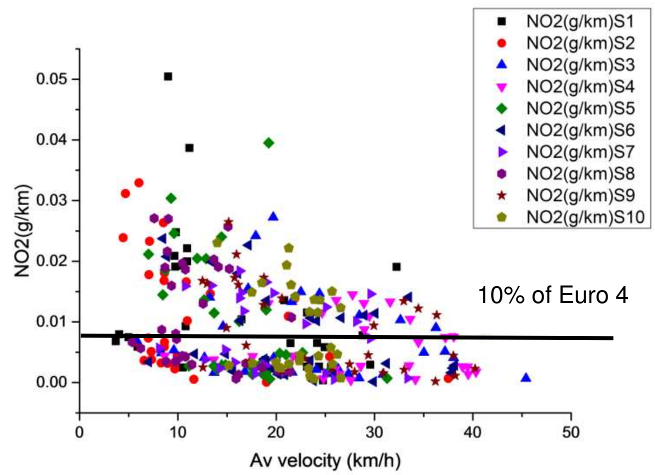

Figure 26. NO_2 emissions for S1-S10 v. the mean velocity.

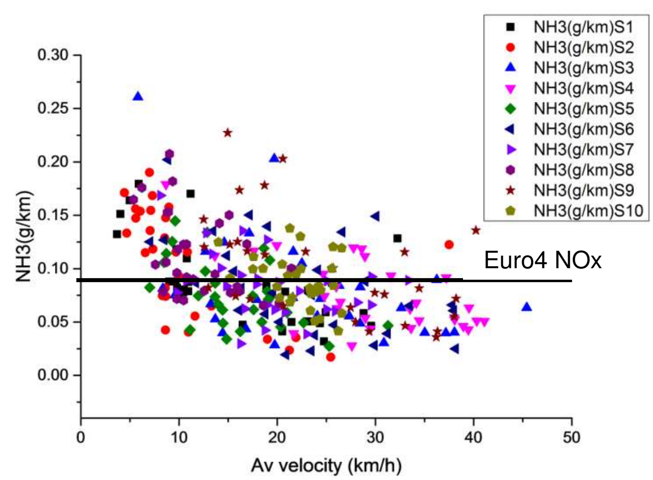

Figure 27. CO_2 emissions for S1 – S10 v. the mean velocity

temperature rise across the catalyst was about 150^{o}C at a maximum, which was reduced, for the more congested test in Fig. 8 to 50^{o}C, later in the journey. During the hot start in congested traffic the engine out UHC and CO were high due to the low powers used and the locally richer mixtures used during accelerations. These contribute to the relative high temperature rise across the TWC in Figs. 8 and 9 and to the high UHC, CO and NO_x emissions for journey S1, that were found in the results presented below.

The Emissions alongside the Roadside Air Quality Monitoring Station, S2 and S9.

The average CO_2, total hydrocarbons (THC), CO and NO_x emissions as g/km are shown as a function of the mean speed for S2 in Figs. 10-13 and for S9 in Figs. 14-17. These two sections are the north and south direction traffic that passes the roadside air quality monitor that exceeds the European air quality standards for NOx and PM at peak traffic times of the day. It was also found, as shown in Figs. 18-21, that the worst traffic emissions were for S1, that contains upstream queuing traffic from the traffic lights at the end of S2. The 290 data points for all 29 journeys over S1 – S10 are shown for the four legislated pollutants in Figs. 22 – 25. All the results show several journeys with mean emissions below the NEDC but the majority of the mean emissions for all four pollutants were above the NEDC for low average speeds caused by the stop/start motion in the congested traffic.

CO_2 Emissions

These results show that congestion was very bad for CO_2 emissions and fuel economy. Fig. 18 shows that for S1 there were only 4 of the 29 journeys where the CO_2 emissions were <180 g/km, as certified on the NEDC for this vehicle. These four journeys occurred for average speeds above 23 km/h. However, there were 5 journeys above 23 km/h with higher CO_2 emissions than 180 g/km. At the lowest mean velocities there were a wide range of journey average CO_2 and Fig. 18 shows for journey section S1 there were journeys where the CO_2 was three times that of the NEDC value and these were in the velocity range 4 – 12 km/h, with a high number of stop/starts.

For the journey section by the road side air quality monitor, S2 and S9, most of the journeys had CO_2 emissions >180 g/km for the NEDC. In Fig. 10 for S2 only three of the 29 data points were below 180 g/km and these were for mean velocities >19 km/h. However, for 22 km/h Fig. 10 shows that there were two journeys with CO_2 emissions above the NEDC value. At low velocities with congested traffic Fig. 10 shows that journey S2 had three trips with three times the NEDC CO_2. Similarly, for the traffic travelling into the city on route S9, Fig. 14 shows that there were five journeys where the CO_2 was below the NEDC value for mean velocities above 28 km/h, but in the speed range 30-40 km/h there were seven journeys with higher CO_2 than on the NEDC. For S9 there was only one journey at 15 km/h that had three times the NEDC CO_2. The CO_2 emissions are thus very dependent on the local traffic conditions which constrain the action of a driver to follow those of the vehicle in front.

For S2 the CO_2 emissions do not meet those certified under the NEDC until the mean velocity was 25 km/h. These low mean velocities and high CO_2 conditions occur with the high traffic flows in the evening period. However, the inward traffic flow is worse for CO_2 in S9, where the mean velocity has to be above 38 km/h before the NEDC CO_2 is reached. The mean velocity on the NEDC is 33.6 km/h and these higher CO_2 at lower mean speeds would be expected from the greater number of stop/starts per km that give rise to the lower mean velocities. For the outward journey, S1 had a mean velocity of 25 km/h before the CO_2 emissions were equal to or less than those certified for the NEDC. However, in the opposite flow of this same section of road, S10, the results were that the NEDC CO_2 was never achieved, as the highest velocity in this section in the 29 repeat journeys was 27 km/h. The was due to the back up of traffic queuing from the next traffic lights towards the city centre in Fig. 1.

THC Emissions

The THC emissions for S2 and S9 by the roadside air quality monitor are shown in Figs. 11 and 15. For S2 the journey mean velocity range was 4 – 38 km/h and all the data was well above the NEDC limit below a speed of 18 km/h. There were five journeys in the speed range 4-8 km/h with greater than five times the NEDC THC. As many of the individual HC that were measured were toxic, such as benzene, 1, 3 butadiene and aldehydes, these exceedances of NEDC standards in low speed congested traffic are a potential health concern. For the S9 section the average speed varied from 12 – 40 km/h and the higher minimum journey speed than for S2 was due to the absence of a traffic light ahead of the flow, as the next traffic lights were about 1km ahead and congestion would only reach the S9 section in the peak early morning traffic flow at 8am. Due to access to the instrumented vehicle no measurements were made at 8am. All the high congestion measurements were undertaken around 5pm and this peaked in the northerly direction on section S2. Fig. 15 shows that for S9 there were only two journeys with the THC less than NEDC values and these occurred at mean speeds greater than 28 km/h. However, there were nine journeys between 28 and 40 km/h that were at or above the NEDC level.

The first journey after the hot start in SI had the highest THC emissions, as shown in Fig. 19. These were higher than for any other journey as shown in Fig. 23. All 29 journeys were greater than the NEDC THC over the velocity range 4 – 32 km/h and nine were greater than five times the NEDC limit. It was shown above that S1 also had the highest CO_2 emissions and it will be shown below that it had the highest CO and NOx emissions. The low powers used at idle in congested traffic lower the exhaust temperature entering the catalyst and increase the engine out THC emissions. The net result was an apparent cold start influence on the THC, even though the catalyst was initially hot. This apparent cold start influence is also shown in the CO and NOx results, as discussed below.

The THC for all 29 journeys for all 10 sections are shown as a function of the mean journey speed for that section in Fig. 23. This shows a very wide variation in THC for the same mean velocity. This was due to differences in the number of stop/starts and the start acceleration magnitude, caused by the presence of other traffic. For most journeys the NEDC THC limit was exceeded and only about 10% of the data was below the NEDC limit and this occurred over the speed range 15 – 45 km/h. But there was more data in the speed range 15 – 40 km/h that had THC greater than the NEDC levels.

The reason for the higher THC in real world driving than on the NEDC are due to several influences. The low engine powers used at the low average speeds in real world driving result in higher engine out emissions. This can result in the oxygen storage of ceria being inadequate to oxidise the HCs during rich excursions and thus leading to HC slippage.

CO Emissions

The CO emissions are shown for the section S2 in Fig. 12 and most of the data was less than the NEDC values apart from in the low mean velocity range of 4-8 km/h where there were 9 journeys with CO above the NEDC. This is in contrast to the THC emissions where most of the data was above the NEDC limit. This difference was due to the lower TWC light off temperature for CO compared with THC. The CO in the southbound traffic in the same section, S9 route, is shown in Fig. 16 and most of the data here is less than the NEDC CO, apart from 9 journeys with CO above the NEDC limit. The data had no correlation with the journey mean velocity. These low CO for the two lanes of travel by the roadside air quality monitor, indicates no problem with enhanced CO emissions.

The CO emissions for the first section of the journey, SI, are shown in Fig. 20 and all 29 journeys were above the NEDC limit. Much of the CO data was four times the NEDC CO limit and some were six times the NEDC limit. This was a similar pattern to the THC data and the reason was that in this first section the catalyst produced hot exhaust temperatures downstream of the TWC but was cool upstream of the catalyst due to the low powers used and the extensive time at idle. Fig. 24 shows that for the other 9 journey sections, the CO was less than the NEDC CO limit. If SI is ignored then only 17% of the rest of the data was above the NEDC limit across the 4 – 35 km/h speed range. The proportion of the data greater than the NEDC CO limit was higher at low speeds, but there were high CO journeys up to 32 km/h. The CO emissions were thus highly dependent on the individual traffic movements, which controlled the movement of the test vehicle in congested traffic.

NO_x Emissions

The NO_x emissions for S2 are shown in Fig. 13 and they were all less than Euro 6 NOx for journey speeds >12 km/h. 38% of the 29 journeys were less than Euro 6 NO_x across all speed ranges. However, there were a significant number of journeys in congested traffic with mean velocities in the range 4 – 8 km/h, with NOx up to two times the Euro 6 NO_x limit. Part of the reason for low NO_x is the low engine powers used in congested traffic, as engine out NO_x increases with increased power, as the peak temperature increases with power. Also at low powers EGR levels are higher which gives a larger reduction in NOx and also reduces CO_2, due to lower pumping power with a more open inlet throttle for the same power.

For the opposite direction journeys on route S9 in Fig. 17, 59% of the 29 journeys had NO_x below Euro 6 levels and 90% were below Euro 4 NO_x levels. This low NO_x occurred for journey average speeds from 12 to 40 km/h. The S9 journeys into the city were less congested than the outward S2 journeys, but this was because the most congested times into the city centre at 8am were not measured. There were three journeys with speeds <20 km/h where the NO_x was very high. On average journeys in S2 and S9 close to the roadside air quality monitor had NO_x emissions at or below the Euro 4-6 NO_x levels, apart from the times of the day with the most congested traffic. The exceedances in NO_2 at the roadside air quality monitor were due to the presence of low speed congested traffic adjacent to the monitors in the morning and evening periods of highly congested traffic.

For the first journey section S1 in Fig. 21 83% of the 29 journeys had NO_x emissions above the Euro 6 emissions level. The NO_x emissions were much higher than for the S2 and S9 journeys and Fig. 25 shows that the SI NO_x was much higher than for all the other 9 journey sections. The reason for this was discussed above, with considerable stop/start and idle events in SI, after the initial short uncongested road section. The exhaust temperatures upstream of the TWC were below the catalyst light off temperature for NO_x until close to the end of section S1. Fig. 25 shows that with the exception of section S1 most of the NO_x emissions for the other sections were below the Euro 6 level. The data above the Euro 6 level were confined to the 4 – 29 km/h mean velocity region and would not be seen on an RDE cycle as these low mean velocities are omitted from the RDE cycles. This is why RDE journeys with gasoline vehicles and lambda 1 TWCs all show no real world effects with the NO_x emissions below Euro 6 levels [18-20, 33].

These NO_x emissions show that SI vehicles will be a significant source of elevated roadside NO_2 in congested traffic, but will not be the dominant source of NO_2. Diesel vehicles are mainly responsible as prior to Euro 6 there was no catalytic deNOx technology and higher engine out NO_x emissons than for SI vehicles was allowed. However, even for Euro 6 diesel vehicles with deNO_x catalysts real world NO_x emissions are substantially greater than on the NEDC [18-20, 33]. This is because Diesel engines have lower exhaust temperatures at the low power of congested traffic and often will be below the 200^oC light off temperature of most deNO_x catalytic systems. Also at high powers, where the exhaust temperature can be $>500^oC$ all deNOx systems have a reduced efficiency, which does not occur for TWC until much higher temperatures. This makes deNOx catalysts perform poorly under low and high power conditions. The RDE test cycle is weighted to high powers and this results in a relatively poor deNO_x performance due to the loss of deNO_x catalyst efficiency at high catalyst temperatures.

DeNO_x systems for diesels are usually selective catalytic reduction (SCR) devices that use a reducing agent, normally urea, which requires a complex control mechanism to achieve proportional urea injection to the upstream NOx concentration. As the transients are greater in real world driving than on test cycles a calibration that is satisfactory for test cycles may not be satisfactory for the greater and more frequent accelerations in real world driving. Thus even with deNO_x catalytic control of NOx, diesel engines will have higher real world emissions than the NEDC emissions and a greater real world effect than for gasoline engines with TWC and lambda one control.

Hadavi et al [7] for a Euro 3 diesel in the same congested section of this journey, S2, measured NOx emissions of 1.9 – 3.0 g/km at mean average velocities of 5.1 – 6.4 km/h. These were between 2.9 and 4.6 times the NEDC level for this vehicle of 0.65 g/km. These diesel emissions at Euro 3 are much greater than for the SI engine in Fig. 25, which for the same mean velocity was about 0.12 g/km, which is over an order of magnitude less than for the diesel results. With deNO$_x$ catalysts for Euro 6 diesel vehicles the regulated NO$_x$ emissions are the same as for Euro 4 SI emissions. However, real world measurement of Euro 6 vehicle emissions [18-20, 33] have shown a major problem of much higher missions than certified, for the reasons discussed above. Both spark ignition and Diesel engines have problems of high emissions at the low powers used in congested low speed driving as shown in this work and in the work of Hadavi et al. [7] for diesels on the same congested road. The main reason for this is low exhaust temperatures and higher engine out emissions at the low average speeds of congested traffic, as shown by Hadavi et al [7] for diesels and Figs. 8 and 9 in the present work. The loss of deNO$_x$ catalyst efficiency at high powers and high exhaust temperatures for SCR catalysts also makes the real world performance poor on the RDE test procedures. This makes diesel vehicles more sensitive to real world driving than for gasoline powered spark ignition engine vehicles, where the main real world problem is for low speed congested traffic real world driving, as highlighted in this work.

NO_2 and NH_3 Emissions

The NO_2 emissions from lambda 1 SI vehicles are normally assumed to be low, but there are relatively few measurements to demonstrate this. The NO_2 emissions measured on the 10 journey sections with 29 repeat journeys are shown in Fig. 26. Most of the data was below 10% of Euro 4 NO$_x$, but there were a number of journeys where the NO_2 was 25% of the total NO$_x$ and this is similar to the proportion in diesel engines [7]. However, the higher total NOx for diesels means that the NO_2 emissions will also be higher even if the proportion is similar to real world congested traffic SI vehicle emissions. Thus the direct contribution of SI NO_2 to roadside NO_2 measurements is significant, but is less than the direct NO_2 emissions from diesels.

The ammonia emissions for all the journeys are shown in Fig. 27 as a function of the mean vehicle speed. The ammonia emissions were high and of the same order of magnitude as the NO$_x$ emissions. Approximately 50% of the ammonia data is higher than the NO$_x$ emissions. There were some journeys where the ammonia emissions were very low.

Ammonia is generated across TWCs by the reaction in Eq. 5.

$$3H_2 + 2NO > 2NH_3 + O_2 \tag{5}$$

This occurs in local rich excursions during acceleration, which generate the hydrogen to react with NO. The large number of accelerations during congested traffic driving results in high NH_3 emissions. The NH_3 have been reduced in Euro 6 SI TWC vehicles through better lambda control and reducing the rich excursions in transients that lead to the NH_3 formation.

Conclusions

1. Emissions from low speed congested traffic are responsible for elevated air pollution at roadside air quality monitoring stations and for air quality exceedances in cities. SI vehicles are a significant contributor to the emissions as well as diesel vehicles.
2. 50% of passenger car journeys in cities are 5km or less [23] in the real world and this should be the distance used for real world emissions studies, as in the present work. The journeys used must also include congested traffic, if air quality issues are to be addressed.
3. The WLTC and RDE test procedures involve higher speeds and no congested traffic driving and in the case of the RDE no cold start. They are thus test cycles which will not produce data relevant to explaining why air quality in cities is improving much more slowly than vehicle test cycle emissions are being reduced.
4. The congested traffic journey studied had a mean vehicle speed range of 4 – 45 km/h, depending on the time of the day and the traffic congestion. The prime reason for high CO_2 emissions in congested traffic was the large number of stop/starts and the low thermal efficiencies at the low engine powers used in low speed congested traffic driving. Hybrid vehicles are particularly suited to reducing the emissions in stop/start congested traffic, as they can used stored energy for the frequent starts and recover part of this energy in the stops.
5. The hot start catalyst temperature was initially 350^{o}C and it took 10s to reach 400^{o}C in the first acceleration. It took between 100 and 400s for the upstream exhaust temperature to reach 400^{o}C after the hot start in congested traffic. The low powers used and the extensive idle periods resulted in low exhaust temperatures and high HC and CO engine out emissions. This combined to give high tailpipe emissions for the first section of the journey after the hot start.
6. The congested traffic emissions of CO were very high relative to the Euro 4-6 levels for mean vehicle speeds <10 km/h. For THC the emissions were high over a wider range of average speeds up to 30 km/h and this was due to the higher catalyst light off temperature for THC compared with CO. Above these speeds the emissions of CO and THC were well below Euro 4-6 levels.
7. The NO$_x$ emissions were lower than the Euro 6 levels for mean vehicle speeds above 25 kph, apart from for the first part of the journey immediately after the hot start. The NOx emissions increased with increase in congestion. This is part of the reason why roadside NO_2 measurements are high during periods of congested traffic.
8. NO_2 emissions were significant in congested traffic driving and were >10% of Euro 4 NO$_x$ and for some highly congested journeys >25% of NO$_x$. Thus SI vehicles are not negligible direct emitters of NO_2. NO_2 formation occurred during lean excursions in severe decelerations.
9. Ammonia emissions were similar to the NO$_x$ emissions, due to rich excursions during acceleration. In this vehicle the calibration of the TWC lambda control was biased 2% rich to maximize NOx reduction, but this created high levels of NH_3.

References

1. Daham, B., Li, H., Andrews, G.E., Ropkins, K., Tate, J.E. and Bell, M.C., “Comparison of Real World Emissions in Urban Driving for Euro 1-4 Vehicles Using a PEMS”, SAE International Technical Paper 2009-01-0941. Also published in: “Emissions Measurement and Testing, 2009”, SAE International SP-2256, pp.129-144. ISBN 978-0-7680-2152-3. SAE International, 2009.
2. Li, H., G.E. Andrews, D. Savvidis, B. Daham, K. Ropkins, M.C. Bell, and J.E. Tate, *Characterization of Regulated and Unregulated Cold Start Emissions for Different Real World Urban Driving Cycles Using a SI Passenger Car.* SAE International Technical Paper 2008-01-1648. 2008.
3. Tziraks, E., K. Pitsas, F. Zannikos, and S. Stournas, *Vehicle Emissions and Drivng Cycles: Comparison of the Athens Driving Cycle (ADC) with ECE-15 and European Driving Cycle (EDC).* Global Nest, 2006. **2006. 8(3)**: p. 282-290.
4. Wang, A., et al., *On-road pollutant emission and fuel consumption characteristics of buses in Beijing. Journal of Environmental Sciences.* 2011. **23(3)**(3): p. 419-426.
5. Wang, X.M., G. Carmichael, D.L. Chen, Y.H. Tang, and T.J. Wang, *Impacts of different emission sources on air quality during March 2001 in the Pearl River Delta (PRD) region.* Atmospheric Environment, 2005. **39(29)**: p. 5227-5241.
6. Wyatt, D.W., H. Li, and J. Tate., *Examining the Influence of Road Grade on Vehicle Specific Power (VSP) and Carbon Dioxide (CO2) Emission over a Real-World Driving Cycle.* SAE International, 2013.
7. Hadavi, A.S., Przybyla, G., Li, H. and Andrews, G.E., *Comparison of Gaseous Emissions for B100 and Diesel Fuels for Real World Urban and Extra Urban Driving.* Proceedings SAE International Powertrain Fuels and Lubricants Conference, Malmo, Sweden, 2012. SAE Paper 2012-01-1674. Also in SAE International J. Engines, 2012. doi:10.4271/2012-01-1674
8. Przybyla, Grzegorz; Hadavi, Seyed Ali; Li, Hu. and Andrews, Gordon E. *Real World Diesel Engine Greenhouse Gas Emissions for Diesel Fuel and B100* SAE Paper 2013-01-1514 doi: 10.4271/2013-01-1514.
9. Hadavi, S., Andrews, G.E., Li, H., Przybyla, G., Vazirian, M. *Diesel Cold Start into Congested Real World Traffic: Comparison of Diesel and B100 for Ozone Forming Potential*. SAE Paper 2013-01-1145 doi:10.4271/2013-01-1145
10. Hadavi, A., Przybula, G., Li, H. and Andrews, G.E., *Diesel Cold Start into Congested Real World Traffic: Comparison of Diesel, B50, B100 for Gaseous Emissions,* SAE Technical Paper 2013-01-2528, 2013.
11. Li, H., G.E. Andrews, D. Savvidis, B.K. Daham, K. Ropkins, M.C. Bell, and J.E. Tate, *Impact of Driving Cycles on Greenhouse Gas (GHG) Emissions, Global Warming Potential (GWP) and Fuel Economy for SI Car Real World Driving.* SAE International Journal of Fuels and Lubricants 2009. Volume 1 (1): p. 1320-1333.
12. Leeds City Council, *Leeds NGT Trolleybus Public Inquiry TWAO Doc. A-08c-1 Air Quality*, 2013.
13. Leeds City Council, *Leeds NGT Trolleybus Public Inquiry TWAO Doc.C-1-8* Leeds Transport Model –Forecasting and NGT Central Case. Jan. 2014.
14. Leeds City Council, *Leeds NGT Trolleybus Public Inquiry TWAO Doc.C-1-3* Leeds Transport Model –Update. Jan. 2014.
15. Li, H. Khalfan, A. and Andrews, G.E., *Determination of GHG Emissions, Fuel Consumption and Thermal Efficiency for Real World Urban Driving using a SI Probe Car*. SAE Int. J. Engines 7(3):2014, doi:10.427/2014-01-1615.
16. Khalfan, A., Li, H., and Andrews, G., *Cold Start SI Passenger Car Emissions from Real World Urban Congested Traffic,* SAE Technical Paper 2015-01-1064, 2015, doi:10.4271/2015-01-1064.
17. Khalfan, A., Andrews, G.E. and Li, H. *Real Driving Emissions in Congested Traffic: A Comparison of Cold and Hot Start*. SAE International SAE 2016-01-2326.
18. S. Hausberger, S., Blassnegger, J., Lipp, S., *Experience with Current RDE Legislation.* Proc. 3rd Conf. on Real Driving Emissions, Berlin, Oct. 2015.
19. Merkisz, J., Pielecha, J. and Fuc, P., *Selected Investigations of Exhaust Emissions Measurements in Vehicle Real Operating Conditions and their Practical Implications.* Proc. Conf. on Real Driving Emissions, Berlin, Oct. 2015.
20. Bielaczyc, P. *A Comparison of RDE Testing with the WLTP as Evaluation Tools for Emissions and Fuel Consumption.* Proc. 3rd Conf. on Real Driving Emissions, Berlin, Oct. 2015.
21. Marotta A., Pavlovic J. et. al., *Gaseous Emissions from Light-Duty Vehicles: Moving from NEDC to the New WLTP test Procedure*. Environmental Science & Technology. http://pubs.acs.org/doi/pdf/10.1021/acs.est.5b01364
22. Williams, R., Hamje, H., Rickeard, D.J., Bartsch, T., Fittavolini, C., Van de Heijing, P., Lehto, K., Gunter, G., Cotijo, J.A., Zemroch, P.J., Samaras, Z.,Dimaratos, A. *Effect of Diesel Properties on emissions and fuel consumption from Euro 4, 5, and 6 European Passenger Cars.* SAE 2016-01-2246.
23. Liu, Z., Ivanco, A., and Filipi, Z.*, Impacts of Real-World Driving and Driver Aggressiveness on Fuel Consumption of 48V Mild Hybrid Vehicle, SAE Int. J. Alt. Power.* 5(2):2016, doi:10.4271/2016-01-1166.
24. https://www.statista.com/statistics/204123/transmission-type-market-share-in-automobile-production-worldwide/
25. icct–The International Council on Clean Transport, ‘European Vehicle market statistics Pocket book 2013’.
26. Daham, B.K., Andrews, G.E., Li, H., Ballesteros, R., Bell, M.C., Tate, J.E. and Ropkins, K. Application of a portable FTIR for measuring on-road emissions, 20 pp. SAE Paper 2005-01-0676. In ‘Emissions Measurement and Testing 2005’ SAE SP-1941, p.171-192, ISBN 0-7680-1586-3, (2005).
27. Li, H., Ropkins, K., Andrews, G.E., Daham, B., Bell, M., Tate, J. and Hawley, G., ‘Evaluation of a FTIR Emissions Measurement System for Legislated Emissions Using a SI Car. SAE Paper 2006-01-3368. Proceedings of the SAE 2007 Powertrain Fluid Systems Conference, Toronto. ISBN 0-7680-1803-X, 2006.
28. Mamakos, A. and Manfredi, U. JRC report 72196 www.epa.gov/OMSWWW/climate/regs-light-duty.htm

29. Varella, R.A. et al. 'Cold running NOx emissons comparison between conventional and hybrid powertrain configurations using real world driving data'. SAE 2016-01-1010
30. Zhai, H.; Frey, H. and Rouphail, N. A., "Vehicle-Specific Power Approach to Emissions Estimates for Diesel Transit Buses." Environmental Scientific Technology, Vol 42, 2008.
31. Reese, R. II, "Progress (and Challenges) along the Path to 2025", presentation at the Engine Research Center 2015 Symposium, University of Wisconsin, Madison, June 2015.
32. Tim Johnson, Corning. Vehicular Emissions in Review. SAE Paper 2016-01-0919*, SAE Int. J. Engines, Vol. 9, Issue 2, June 2016.*
33. Weiss, M., et al. *Will Euro 6 reduce the NOx emissions of new Diesel cars? Insights from on-road tests with PEMS.* Atmospheric Env. 62, 2012, 657-666. doi.org/10.1016/j.atmosenv.2012.08.056

Contact Information

Professor Gordon E. Andrews, Clean Combustion Research, School of Chemical and Process Engineering, The University of Leeds, Leeds, LS2 9JT, UK.
profgeandrews@hotmail.com
Ahmad Khalfan, Clean Combustion Research, School of Chemical and Process Engineering, The University of Leeds. Email: ml09amk@leeds.ac.uk.

Dr. Hu Li, Clean Combustion Research, School of Chemical and Process Engineering, The University of Leeds. Email: fuehli@leeds.ac.uk.

Acknowledgments

Ahmad Khalfan would like to thank Kuwait government for a PhD scholarship to support his study at Leeds University. Data used in this paper were collected during an EPSRC funded project RETEMM (Real-world Traffic Emissions Measurement and Modeling) and thus thanks go to EPSRC and the RETEMM team, specifically for Dr. James Tate and Dr. Karl Ropkins who were part of the team.

Definitions/Abbreviations

A/F: Air Fuel ratio
EI: Emissions Index
FTIR: Fourier Transform Infrared.
FTP: Federal Test Procedure.
GHG: Green House Gas.
GPS: Global Positioning System.
GWP: Global Warming Potential
LHC: Leeds Headingley Cycle
NEDC: New European Driving Cycle.
OBS: On Board Emissions Measurement System.
SI: Spark Ignition.
TAPs: toxic air pollutants.
TWC: Three Way Catalyst.
UDC: Urban Driving Cycle.
EUDC: Extra Urban Driving Cycle
WLTC: World Light-duty Test Cycle.